Original scientific paper
Received:01.09.2025
Accepted:10.11.2025
UDC: [674.053:534.322.3]:[621.389.08:004.4.032.26]

MACHINING ACOUSTICS: SIGNAL PROCESSING AND DEEP LEARNING AS A TOOL FOR PROCESS MONITORING

Srđan Svrzić[1]

[1]Associate professor, Department of Wood Technology,
Faculty of Forestry, Belgrade University, Serbia
e-mail: srdjan.svrzic@sfb.bg.ac.rs

ABSTRACT

The requirements of Industry 4.0 and beyond go hand in hand with adaptive, intelligent process control through the application of some form of AI. To this end, some acoustic phenomena have been observed in this series of research conducted over the last few years. Noise analysis for different working conditions of circular saw blades was investigated in this study. The main objective of this work was to verify the existing relationships between the recorded noise patterns and the corresponding operating conditions of different circular saw blades. This goal was achieved by analysing noise signals and using different neural network architectures, such as GoogleNet, MobileNetV2, VGG19, DenseNet, SqueezeNet, ResNet and InceptionV3. The results obtained in this series of investigations suggest that the noise generated during cutting can be used as a tool for process monitoring with high accuracy. Various cases are presented in this paper, such as determining the speed of the same saw, recognising different types of saws idling at different speeds, recognising types of wood being processed with the same saw, and idling the same type of saw at different bluntness and utilisation. In all cases presented, the trained neural networks showed a relatively high accuracy in determining the observed output.

Keywords: acoustic signal, circular saw blade, wood machining, process monitoring, decision making, deep learning network.

1. INTRODUCTION

When several bodies or media interact with each other, sound is inevitably generated. It is regarded as a mechanical wave that propagates through the surrounding medium, such as gas, liquid or solid. By definition, sound is a longitudinal wave that represents fluctuations in the pressure or density of the conducting medium. Sound can be defined as a signal, i.e., it carries information, such as speech. It is determined by amplitude, frequency and duration. Sound is often equated with noise, i.e., if a sound has no recognisable pattern, it is classified as noise.

A tool (circular saw blade) behaves like a noise source, either when idling or when cutting. In the first case, it behaves like a vibrating guitar string which, depending on the speed, the number of teeth and the geometry of the teeth, produces a sound that is often referred to as whistling. In the second case, additional noise is generated by the interaction between the tool and the material, which is strongly influenced by the properties of the material itself. The noise generated during woodworking comes from four possible sources: the machine motor, the gearbox, the whistling of the tool and the interaction between the tool and the material. These noises cannot be observed separately during processing. The interaction between tool and material leads to an increased load on the motor and influences the whistling of the tool, so that a comparison of the noise when idling and the noise during cutting is pointless.

In recent decades, many authors have addressed the possibility of using noise as a means of process monitoring. This is important from the point of view of carrying out the cutting process within the specified optimum parameter limits, the surface quality, the possible exceeding of the power used or the blunt condition of the tool.

Different types of broadband frequency sensors (Nasir et al. 2019, Tanaka et al. 1992, Aguilera et al. 2007) or microphones (Cyra and Tanaka 2000, Iskra and Tanaka 2005, 2006, Iskra and Hernández 2012, Aguilera et al. 2016, Miric-Milosavljevic et al. 2023) were used for sound and acoustic emission (AE) measurements. In addition, the sound recordings were processed using MATLAB software (Nasir et al. 2019, Mandic et al. 2015, Miric-Milosavljevic et al. 2023).

Both power consumption and sound or AE signals provide inputs for process control and monitoring (Goli et al. 2010, Aguilera and Zamora 2007, Aguilera and Barros 2010, 2012, Aguilera 2011a).

While cutting force (Naylor et al. 2012, Porankiewicz et al. 2011, Goli et al. 2018) and power consumption (Kovač et al. 2021) have been evaluated as factors that strongly depend on selected cutting parameters, some authors did not find a strong relationship between noise and other sawing and milling factors (Szwajka et al. 2008) and mostly concluded that AE signals gave worse results than power measurements (Jemielniak et al. 2011), while some others only investigated sound pressure level as an output. It is important to emphasise that most of the work focused on milling.

The progression of tool bluntness during milling was also investigated using sound pressure measurements (Aguilera et al. 2016) and provided satisfactory results.

However, the frequency, time domain and intensity analysis was performed by a few authors (Mohring et al. 2019, Nasir et al. 2019, 2020 and 2021). The noise represents a three-dimensional signal and must therefore be observed in this way. A simple amplitude or sound pressure analysis cannot provide satisfactory input for further processing or relevant considerations. This method provided a comprehensive picture of the sounds generated during cutting with different tools that allow further analysis and the implementation of different artificial neural networks (ANN) to monitor the whole process.

Various signal processing techniques using time and frequency analyses are used to determine the effects of the cutting parameters. The monitoring of the machining process, predictions and decision-making can be achieved by some AI technologies such as artificial neural networks (ANN), fuzzy logic and neuro-fuzzy inference systems (Abellan-Nebot and Subirón 2010). The prediction of tool wear (Szwajka et al. 2008, Zbieć 2011, Zafar et al. 2015) and the prediction of parameters (Iskra and Hernández 2012) were achieved using the ANN approach. The modelling and prediction of surface roughness was also performed using ANN (Iskra and Hernández 2009 and 2012, Tiryaki et al. 2014, Stanojevic et al. 2017).

Deep learning networks, or more generally, AI approaches in wood research, are used for wood identification (Sun et al. 2021, de Geus 2020), wood fibre segmentation (Kibleur et al. 2022), wood processing and tool monitoring (Nasir and Sassani 2021, Jegorowa et al. 2021) and classification of processing parameters (Svrzic et al. 2023). The basic idea of AI implementation is to create a tool that can be used to make decisions that can lead to more efficient production processes. In order to achieve intelligent production, the collected data must be transformed in such a way that it is suitable for the deep learning process. In general, there are some rules for the preparation of raw data: 1) The data must be suitable for the network architecture; 2) the dimensionality must be reduced so that the patterns are more recognisable; and 3) the data must be prepared in such a way that it covers the entire solution space.

Regarding the scope of this article, particular attention has been paid to the acquisition and analysis of sound signals (also in terms of measuring cutting performance), especially considering that there is still much room for theoretical, experimental and even more practical applications in the field of woodworking. The global market for woodworking machinery was estimated at $4.72 billion in 2022 and is expected to grow from $4.86 billion in 2023 to $6.80 billion in 2030 (Fortune Business Insight 2023). The proposed approach to process control can increase the applicability and commercial value of the machine and thus contribute to the global market.

2. MATERIALS AND METHODS

The Freud LU1C 0100, Freud LU2B 0500 and Freud LU2C 1200 circular saw blades were used for this study (Fig. 1 a, b and c). The corresponding numbers of teeth were 22, 48 and 80, respectively. The saw blade LU1C 0100 and the other two have a diameter of 250 mm, an inner diameter of 30 mm, a cutting width of 3.2 mm and a body thickness of 2.2 mm. The carbide-tipped teeth form of the LU1C 0100 is ATB with a positive cutting angle of 10° (Table 1). According to the manufacturer, this blade is intended for longitudinal and cross cuts in solid wood. The LU2B 0500 blade has ATB-shaped carbide teeth with a positive cutting angle of 10° and is intended for cutting solid wood and wood-based materials. The third saw blade is the LU2C 1200 with tungsten carbide (TC), ATB-shaped teeth and a positive cutting angle of 15°. It is designed for rip and cross cuts in softwood, hardwood and wood-based materials.

(a) (b) (c)

Figure 1. *FREUD (a) LU1C 0100; (b) LU2B 0500; (c) LU2C 1200 circular saw blades.*

Table 1. *The tool and cutting conditions.*

Cutting tool	LU1C0100 (Freud)	LU2B 0500	LU2C 1200
Cutting speed	4000 min^{-1}	2000/3000/4000	4000 min^{-1}
Feed rate	10 m/min.	-	-
Teeth shape	ATB	ATB	ATB
Number of teeth	22	48	80
Diameter (mm)	250	250	250
Body thickness b (mm)	2.2	2.2	2.2
Cutting width B (mm)	3.2	3.2	3.2
Rake angle (°)	20	20	18
Clear angle (°)	15	13	5
Inclination angle (°)	10	10	10
Tool override (mm)	10	-	-

Table 2. *Material conditions.*

	Beech	Fir
Moisture content (avg.) (%)	8.16	8.65
St. Dev	0.41	0.14
Wood density air dry (avg.) (g/cm^3)	0.71	0.42
St. Dev	$2.6*10^{-2}$	$3.7*10^{-3}$
Wood density oven dry (avg.) (g/cm^3)	0.69	0.40
St. Dev	$2.5*10^{-2}$	$4.4*10^{-3}$

In one phase of this study, boards of beech (Fagus moesiaca) and fir (Abies alba) measuring 1000 mm × 500 mm × 35 mm were cut. The number of boards was 12, and the total number of cuts was 480 for each species. The cutting tool utilised was the LU1C 0100 circular saw blade, which is intended for cutting solid wood both longitudinally and crosswise.

The study was conducted in the Laboratory of Machines and Apparatus at the Faculty of Forestry, University of Belgrade (Belgrade, Serbia). The machining system used for this study was a Minimax CU 410K combined machine (SCM, Rimini, Italy) equipped with a 3 kW three-phase asynchronous motor. The speed of the motor was set by a customised frequency controller to 4000 rpm with a corresponding frequency of 50.5 Hz. The noise occurring when the tool was idling was recorded using a dbx RTA-M measurement microphone with an electret condenser on the back (Fig. 2a). The RTA-M is an omnidirectional, low-profile frequency measurement microphone specifically designed to record all frequencies from 20 Hz to 20 kHz, ensuring accurate "real-time" "pinging" analysis of the audio signal. It is operated with phantom power. To reduce the effects of vibration, the microphone is housed in a vibration-damping rack. The Focusrite Scarlett SOLO USB audio interface (Fig. 2b) was connected to a PC. Audacity, a cross-platform open-source audio software, was used to record the audio signals. The recordings were sliced and trimmed using the WavePad Sound Editor developed by NCH Software. The measurements were carried out at a sampling rate of 44100 Hz.

Figure 2a. *RTA-M Measurement microphone.*

Figure 2b. *Scarlet SOLO audio interface.*

The microphone was placed 1200 mm away from the rotating tool. The Dino-Lite Edge USB microscope with 470x magnification was used for visual observation of the tool condition in the case of the LU2C 1200 saw (Fig. 3).

Figure 3. *Dino-Lite Edge USB microscope.*

The investigation was divided into the following sections:

1. The idle rotation of the LU2B0500 saw at three different speeds (2000, 3000 and 4000 rpm);

2 The idle rotation of three different saws (LU1C 0100, LU2B 0500 and LU2C 1200) at the same speed (4000 rpm);

3. Cutting beech and fir wood with the LU1C 0100 saw at the same speed (4000 rpm);

4. The idle rotation of the LU2C1200 saw with different degrees of bluntness at the same speed (4000 rpm).

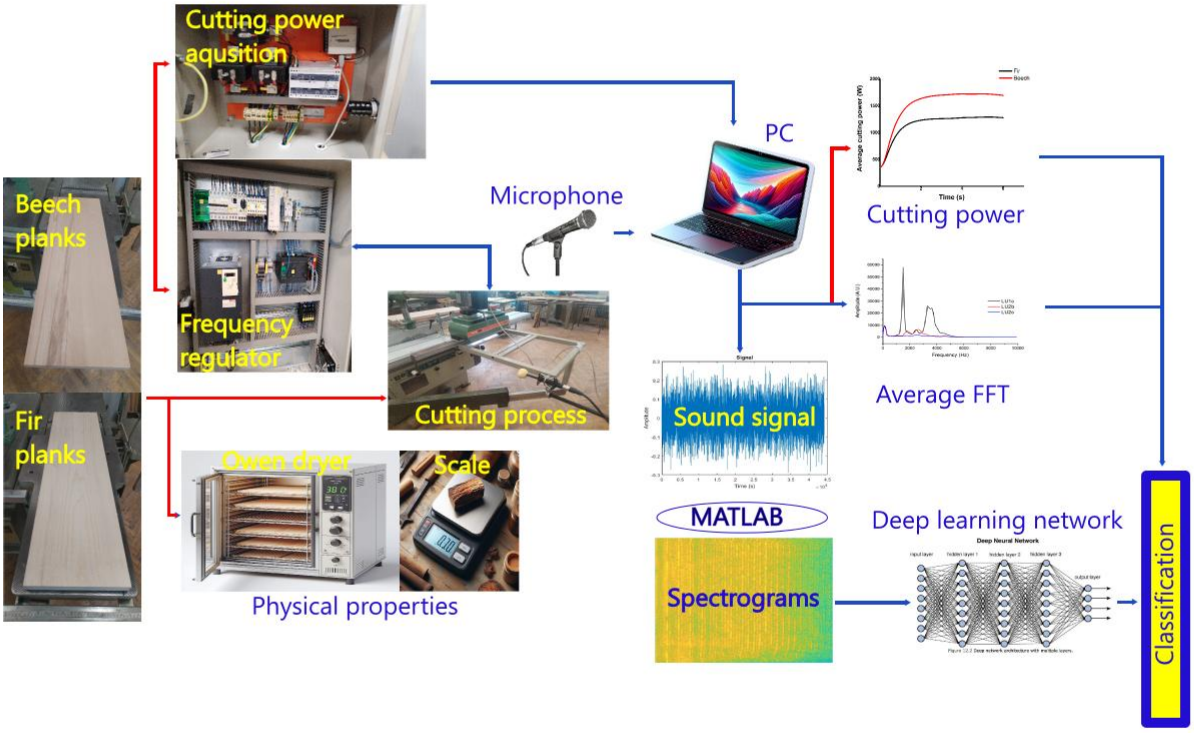

Figure 4. *Experimental flowchart.*

The experimental flowchart of the research carried out is shown in Fig. 4. The blue arrows show the processes in experimental sections 1, 2 and 4, while the red arrows represent section 3.

The device has a Circutor CW-TAN active power transformer for unbalanced three-phase systems with the following characteristics: alternating current 5 A, alternating voltage 230 V, frequency 50 Hz, accuracy 0.5% and analogue voltage output 0-10 V (Mandić et al. 2011). The possible measuring ranges are 5, 10 and 15 kW. The measured cutting power data are given in watts. The operator selects the expected range for a better resolution of the results. The entire system is based on the Power Expert software platform, and the sampling rate has been set to 1000 Hz. The device is also suitable for mobile use. The rotational speed of the saw blade has been set to 4000 rpm with the frequency controller connected to the machine's electric motor. The drive electric motor provides the energy for the interaction between the tool and the wood and for overcoming any friction that occurs between the moving parts of the machine.

$$P_C = P_T - P_I\ (W) \quad (1)$$

Where: P_C - useful power engaged for wood cutting, P_I – machine parts friction overcoming power (idle power), and P_T – total power. The power consumption used in this work was the useful power P_C.

The sounds produced during the experiment came from moving machine parts (electric motor, bearings, spindles, etc.) and from the whistling of the saw blade. These sounds were captured with the microphone and recorded on the PC as wave files. Originally, the length of the wave files was 4 minutes for each saw blade speed. Spectral analysis was performed on these recordings using the fast

Fourier transform (FFT) and the short-time Fourier transform (STFT). On these recordings, spectral analysis was performed using FFT and STFT. The following set of equations describes FFT.

$$F_k = \sum_{l=0}^{N/2-1} \left(g_i W^{ik} + h_i W^{(l+N/2)k}\right) \quad (2)$$

$$F_{2k} = \sum_{l=0}^{N/2-1} (g_i + h_i)(W^2)^{lk} \quad (3)$$

$$F_{2k+1} = \sum_{l=0}^{N/2-1} [(g_i - h_i)W^l](W^2)^{lk} \quad (4)$$

In these equations, N is a number of samples, hi and gi equal sets of samples, $W=e^{-j\Omega T}$ and F_k is the Fourier series for discrete Fast Fourier Transformation (FFT). For N/2 even and N/2 odd samples, the expressions in Eqs. 3 and 4 could be regarded as discrete Fourier transformations (DFTs). The number of iterations required for completing the process described in Eq. 3 is $N\log_2 N$. The short-time Fourier transform, or short-term Fourier transform (STFT), is a natural extension of the Fourier transform in addressing signal non-stationarity by applying windows for segmented analysis. In practice, the procedure for computing STFTs is to divide a longer time signal into shorter segments of equal length and then compute the Fourier transform separately on each shorter segment. The sound/noise signals thus transformed could present the starting point for alternative machining systems and process monitoring and for introducing smart machining.

The use of just FFT was not enough for detailed analysis because the obtained power spectrum involved lots of noise or parasitic frequencies. Further implementation of wavelet transformation, involving Daubechies wavelet, thus obtaining a spectral density graph, significantly smoothened the spectral line, thus pointing to which spectral areas are to be carefully observed. This is particularly important for creating inputs to databases for deep learning networks. Wavelet transform could be described by the following equations:

$$\Psi_{a,b}(t) = \frac{1}{\sqrt{a}} \Psi\left(\frac{t-b}{a}\right) \quad (5)$$

$$W_\Psi(f)(a,b) = \langle f(t), \Psi_{a,b}(t) \rangle \quad (6)$$

Where Ψ presents the mother wavelet with its parameters *a* and *b*, which present the trimming and sliding of the wavelet, respectively; *W* is the wavelet transform function, and *f* is the time domain data function.

A further step was the creation of a database for training deep learning networks. All of the sound signal recordings were transformed into 2D images of 3D spectrograms accomplished by MATLAB R2023 edition. Spectrograms are 3D (frequency-time-power) charts obtained by STFT or wavelet transform of original sound signals. The 2D presentation involves an RGB scale to present the power of certain peaks or spectral areas.

The process of creating spectrograms is known as Gabor transform, and it is intended for making time-frequency plots. The main idea is convoluting the window function (Gaussian function of different lengths) with the time series data function:

$$G(f) = \int_{-\infty}^{\infty} f(\tau) e^{-j\omega\tau} \cdot g(t-\tau) d\tau \quad (7)$$

Where *G* is the Gabor transform, *f(τ)* is the data function, and *g* is the window function.

A further step consisted of cutting the entire 4-minute recording into smaller, even parts of 1 second in length, which was done using the WavePad software. Now it was possible to create a database for training the deep learning network. The first step was to import all 240 short-time recordings of the sound signal for each saw blade speed and convert them into 2D images of 3D spectrograms. Spectrograms are 3D plots (frequency-time-power) obtained by STFT or wavelet transform of the original sound signals. In the 2D representation, an RGB scale is used to represent the power of specific peaks or spectral regions. These 2D spectrograms were saved in the JPG format and served as training data for the deep learning networks GoogleNet, MobileNetV2, VGG19, DenseNet, SqueezeNet, ResNet and Inception V3, which were developed specifically for image recognition. All the implementation was done by using the Python 3.7.4 programming language, along with the PyTorch 1.6.0 and Torchvision 0.7.0 libraries with the CUDA 10.2 GPU drivers. All the computations were done on the workstation with the AMD Threadripper 3970X (32 cores, 3.79 GHz processor), 128 GB RAM and two Titan RTX (24 GB) + NVLink GPUs.

4. RESULTS AND DISCUSSION

The examples of the recordings in wave format for different phases of the experiment are shown in Fig. 5. They have different shapes, indicating different sound intensities, but do not provide sufficient data for classification or any kind of analysis. These audio files were subjected to an FFT to extract specific frequency ranges that could indicate signal changes in order to distinguish different working conditions. The graphs of the FFT for specific cases show the average values of the signal intensities for specific frequencies, excluding the time domain (Fig. 6).

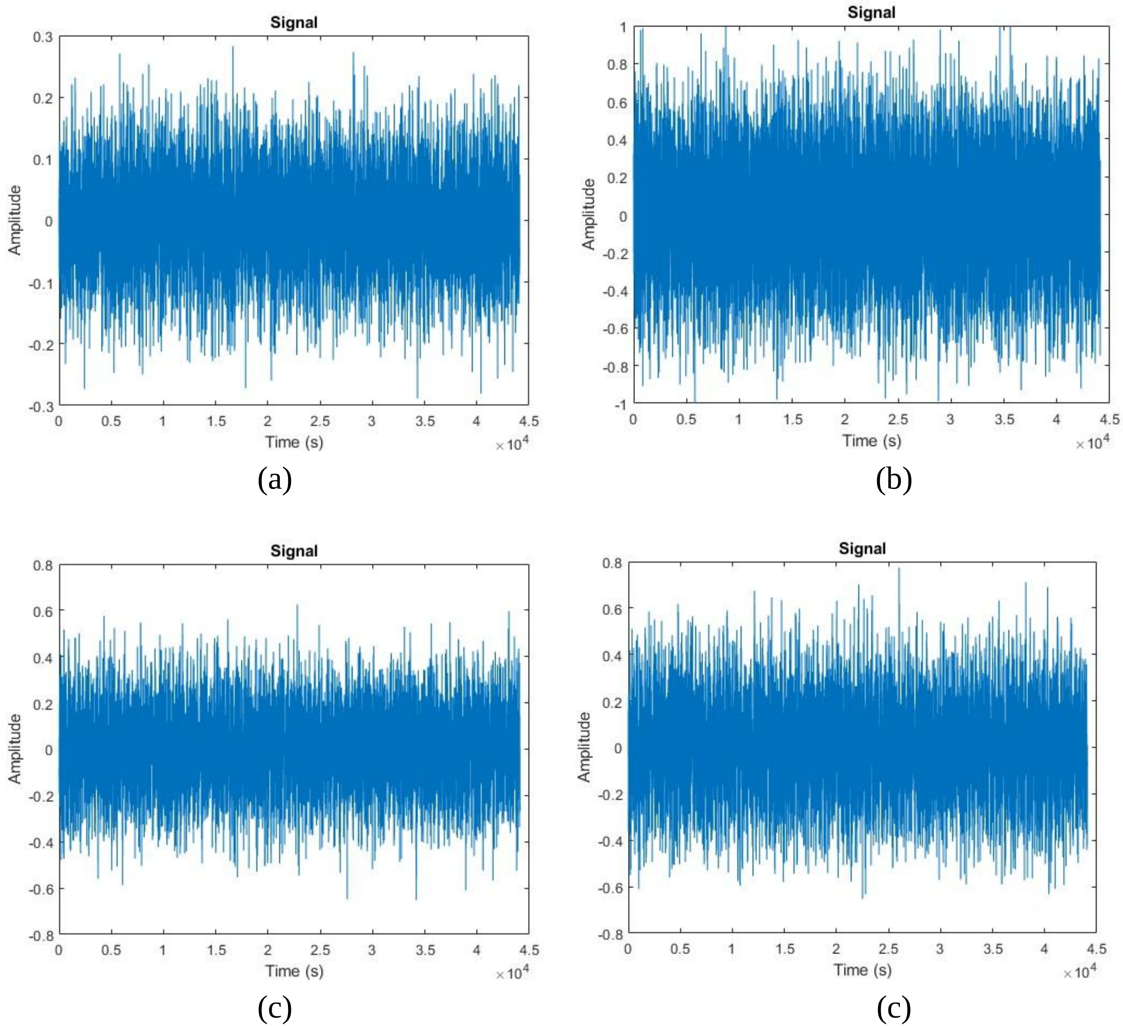

Figure 5. *Example of wav format recordings for: (a) LU1C 0100 at 3000 rpm; (b) LU1C 0100 at 4000 rpm; (c) LU2B 0500 at 4000 rpm and LU2C 1200 at 4000 rpm.*

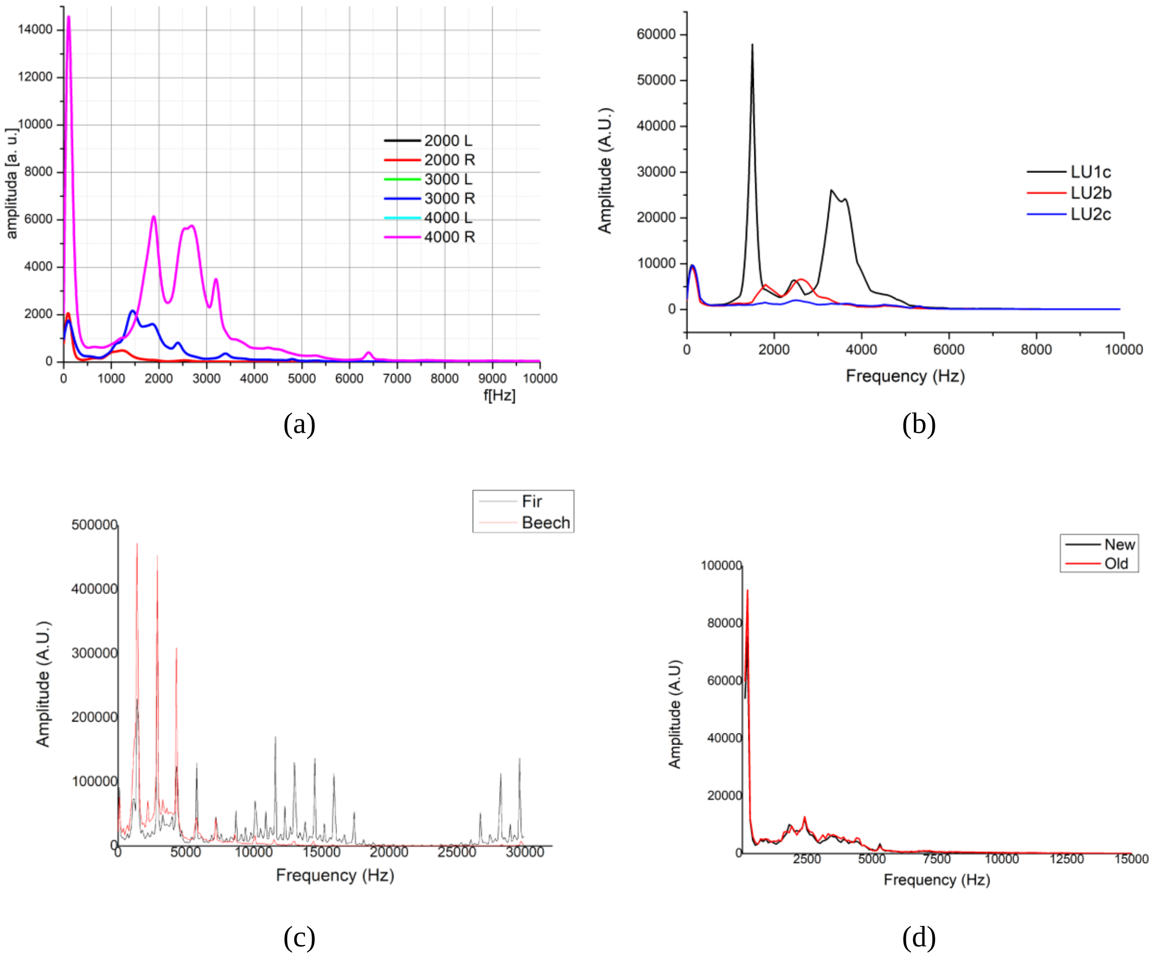

Figure 6. *Average FFT for: (a) LU1C 0100 at three different speeds; (b) LU1C 0100, LU2B 0500 and LU2C 1200 at same speed, (c) LU1C 0100 when cutting beech and fir wood and (d) new and used LU2C 1200.*

In most cases of the average FFT, the graphs behave in very different ways. The most obvious examples are the idling noise of the LU1C 0100 at three given speeds and the idling noise of all saws at the same speed (Figs. 6a and b). The less noticeable differences are found in the idling noises of the new and the old LU2C 1200 saw (Fig. 6d). The legend in Fig. 6 (a) with the markings L and R stands for the left and right recording channels, which are identical, so that there are only three lines: purple for 4000, blue for 3000 and red for 2000 rpm. The spectral ranges between 0 and 500 Hz show very pronounced peaks at all speeds, which increase as the speed of the processing system increases. These peaks are due to the noise generated by the machine itself – the rotation of the electric motor, spindle and gearbox. Another interesting spectral range is between 1000 and 3500 Hz. At these frequencies, a clear increase in the signal can be recognised, which is due to the rotation of the circular saw blade. This assumption is based on simple maths: 2000 revolutions per minute correspond to approximately 66 revolutions per second; multiplied by 48 saw blades results in a frequency of approximately 1600 Hz. At 3000 revolutions per minute, the frequency is 2400 Hz, and at 4000 revolutions per minute, the frequency value is 3168 Hz.

Taking into account the three-column problem and according to Fig. 6 (b), it was possible to extract two spectral ranges that were of interest for further analysis. The first spectral range extended from 0 to about 700 Hz with a peak at 100 Hz. The curves for all three saw blades observed overlapped in this range. As previously mentioned (Svrzic et al. 2023), this spectral range could be related to the noise generated by the machine itself. Since the speed was the same for all saw blades, the curves overlapped completely. The second spectral range of interest is from about 1000 Hz to about 5000 Hz. The spectral density curves for all three saw blades showed different behaviour in this range and resulted in different peak values, especially in the case of the LU1C saw blade. This spectral range was associated with the noise generated when the observed circular saw blades are idling. As can be seen from Fig. 6(c), the sound intensities for beech are significantly higher in the spectral range from 0 to about 4500 Hz. This is consistent with previous studies (Miric-Milosavljevic et al. 2024), in which the idling noise of the same circular saw blade was analysed and in which these frequencies were also found, but with an order of magnitude higher intensity. Some of the peaks in the spectral density diagram are particularly interesting. At a frequency of 1400 Hz, the peak for beech is 472000 (A.U.), which is more than twice as high as 230000 (A.U.) for fir. A slightly smaller divergence occurs at 2900 Hz. At this spectral point, the intensity was 453000 (A.U.) for beech and 439000 (A.U.) for fir. The most interesting intensity peak was found at 4300 Hz, where the intensity was 309000 (A.U.) for beech and 124000 (A.U.) for fir, as this peak was completely absent in previous studies (Miric-Milosavljevic et al. 2024). Some high-frequency overtones occurred in fir but not in beech in the spectral ranges from 7500 to 17500 Hz and from 26000 to 30000 Hz. The reason for this is not entirely clear. One possible explanation lies in the different macroscopic structures of the selected wood species. As a softwood, fir consists mainly of tracheids (91%), which are considerably longer than the tracheids and libriform fibres of beech. The proportion of cellulose, which has a large proportion of crystalline structure, is also significantly higher in fir wood than in beech wood. In particular, the microfibril angle in the S2 layer of the cell wall is considered an important factor for sound propagation in wood (Brémaud 2012). Compared to most hardwoods, softwoods have a very homogeneous cell structure and uniseriate rays. The transition of waves from tracheid to tracheid without the strong influence of vertically orientated rays can be seen as a key factor for wave propagation in fir. This leads to the conclusion that the high-frequency waves in the sound spectrum of fir wood are mainly the result of wave propagation from tracheid to tracheid (Dünisch 2017).

The average FFT for new and used LU2C 1200s is similar, with peaks at low frequencies below 500 Hz and other interesting peaks in the spectral range from 1500 to just above 5000 Hz. In this case, the differences in the waveform are not as obvious as in the previous cases.

However, the average FFT offers no insight into the time scale. As already mentioned, the peaks shown in Fig. 6 (a), (b), (c) and (d) are merely average values at specific points in time. Considering the cyclical nature of the sounds generated during the experiment, the overall picture is somewhat blurred. The STFT is a logical step in visualising the sound signals obtained.

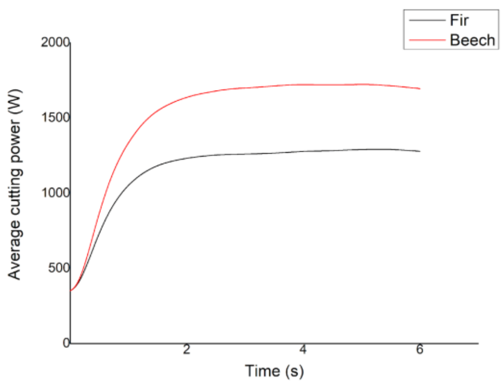

Figure 7. *Average cutting powers for beech and fir wood.*

Power consumption was also measured when cutting beech and fir wood. The average values of the cutting performance for beech and fir wood are shown in Fig. 7. As expected, the average value of the cutting performance for beech is about 50% higher than for fir.

In Fig. 8 (a), the photo under the microscope shows a brand new, unpackaged circular saw blade. It can be seen that the teeth edges and surfaces are in perfect condition, while the same image (b) of a used tool shows cracked edges, traces of corrosion and material deposits on the lateral teeth surfaces.

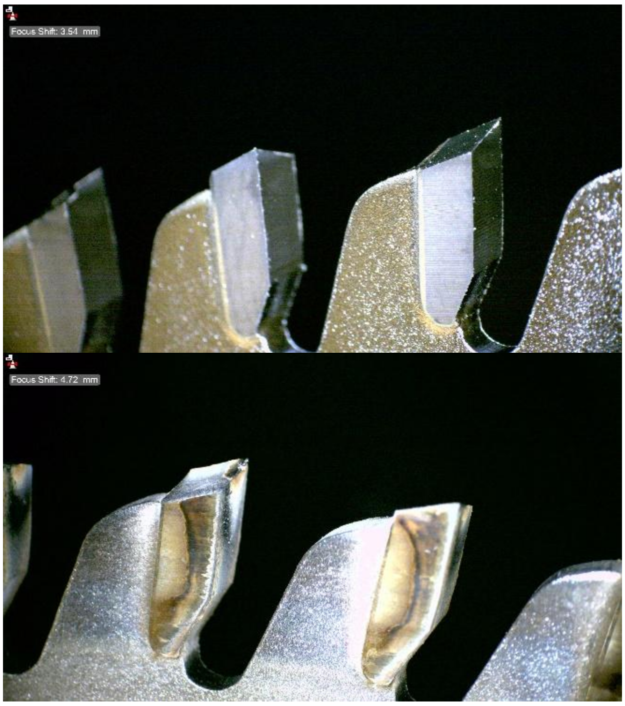

(a) (b)

Figure 8. *Microscopic picture (a) new blade; (b) used blade of LU2C 1200.*

The next step in data processing was to create suitable inputs for ANN. The input data for deep learning networks are spectrograms (see Figs. 9 to 13). The spectrograms were divided into an appropriate number of folders (one for each category according to the number of factors).

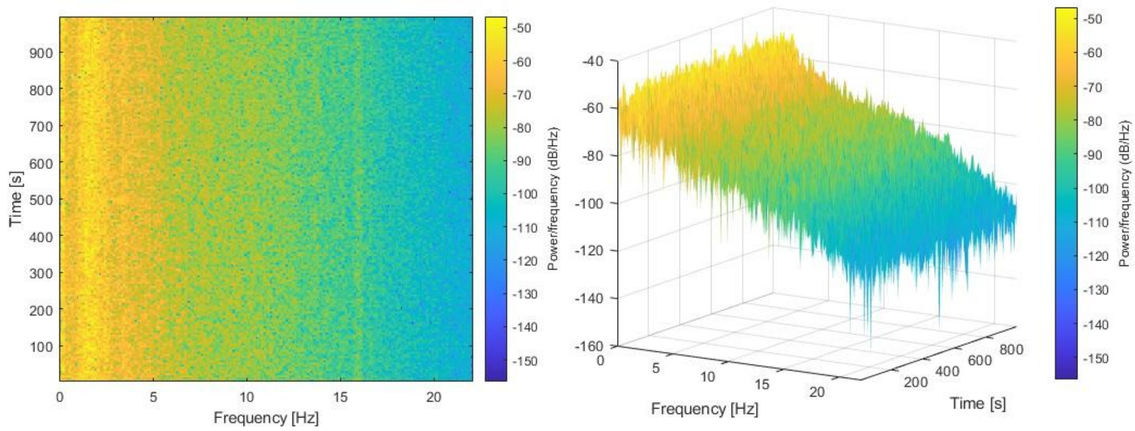

(a) (b)

Figure 9. *Spectrograms presented in (a) 2D and (b) 3D.*

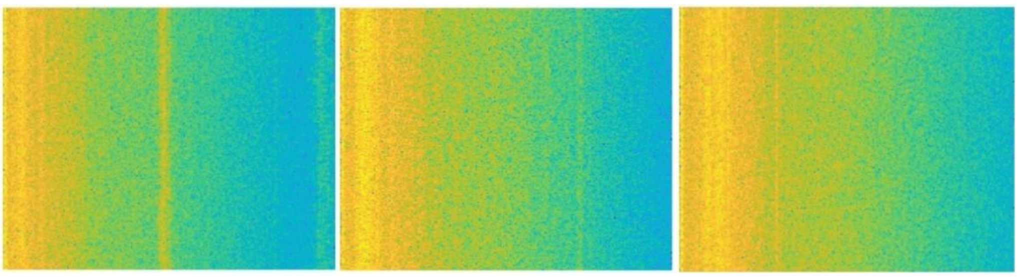

(a) (b) (c)

Figure 10. *Adjusted spectrograms for LU1C 0100 at: (a) 2000 rpm (b) 3000 rpm and (c) 4000 rpm.*

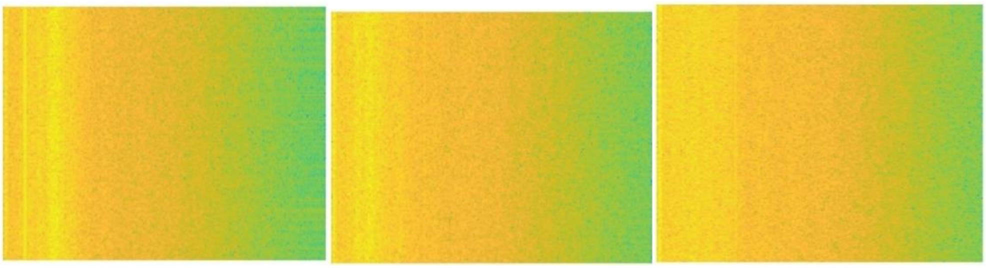

(a) (b) (c)

Figure 11. *(a) Spectrogram without tick and axes for processed sound signal for the LU1C circular saw blade; (b) Spectrogram without tick and axes for processed sound signal for the LU2B circular saw blade; (c) Spectrogram without tick and axes for processed sound signal for the LU2C circular saw blade.*

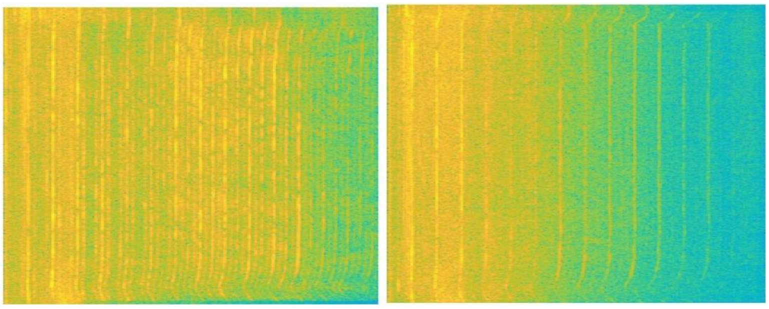

(a) (b)

Figure 12. *Sound spectrograms for: (a) fir and (b) beech wood.*

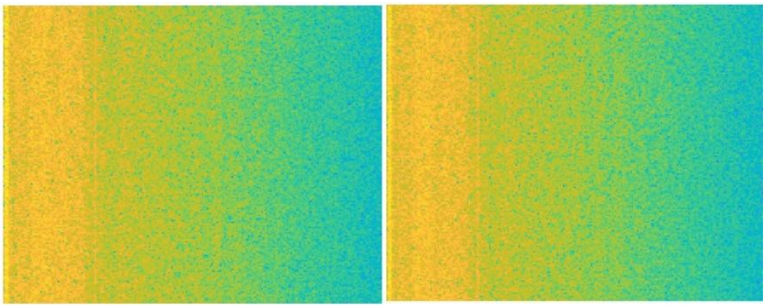

(a) (b)

Figure 13. *Spectrograms for LU2C 1200 (a) new; (b) used circular saw blade.*

The metrics selected for the evaluation and comparison of the developed models included:

$$Accuracy = \frac{T_p+T_n}{T_p+F_p+T_n+F_n} \quad (8)$$

$$Precision = \frac{T_p}{T_p+F_p} \quad (9)$$

$$Recal = \frac{T_p}{T_p+F_n} \quad (10)$$

$$f_1 score = 2\frac{Recal*Precision}{Recal+Precision} \quad (11)$$

where T_p are true positive classifications, T_n are true negative classifications, F_p are false positive classifications and F_n are false negative classifications.

The results for the trained networks are shown in Figs. 14 and 15 and Tables 3 and 4. To analyse the idle noise (research stages one and two), the GoogleNet network was chosen for selected tools, while six different networks were used for the other stages: MobileNetV2, VGG19, DenseNet, SqueezeNet, ResNet and Inception V3.

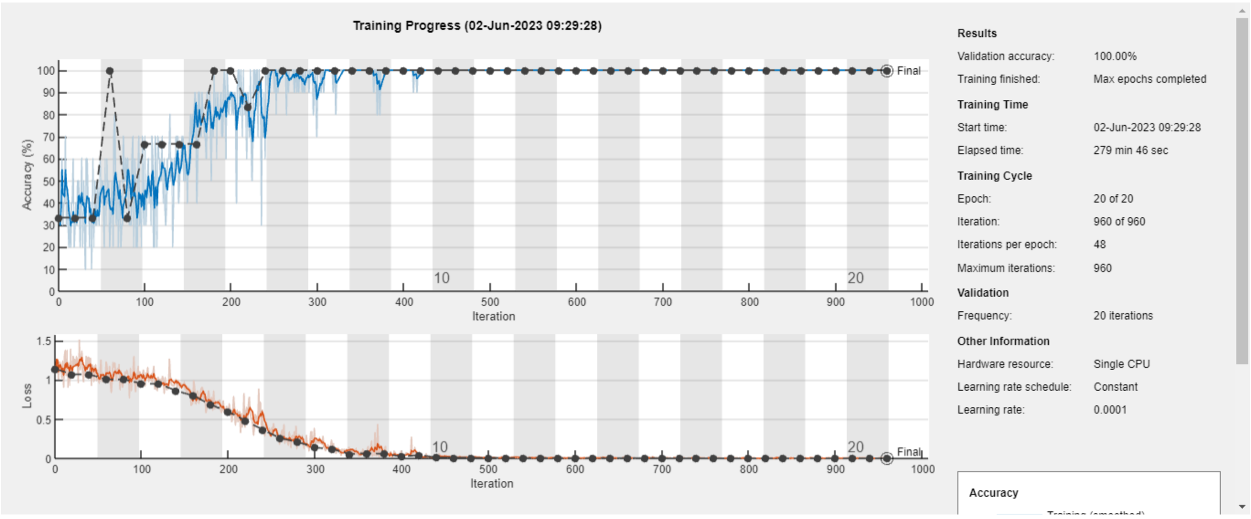

Figure 14. *Deep learning process report (single blade different rotational speeds).*

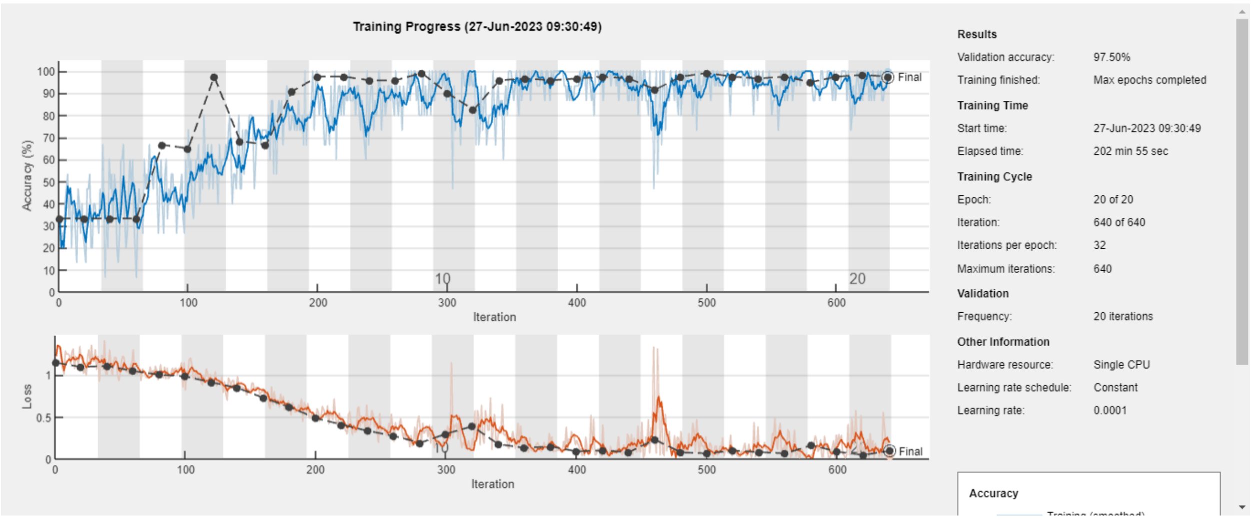

Figure 15*. Deep learning network report (three different blades at same speed).*

The validation accuracy for testing and decision-making for a single tool spinning at three different speeds was 100%, and for three different tools spinning at the same speed, it was 97.5%, all this according to GoogleNet ANN.

Table 3. *Performances of the developed deep learning models for machining sound classification.*

	MobileNetV2	VGG19	DenseNet	SqueezeNet	ResNet	Inception_v3
Accuracy	**0.980**	0.960	0.950	0.950	0.970	0.940
Precision	**0.980**	0.942	0.941	0.959	0.980	0.958
Recall	**0.980**	0.980	0.960	0.940	0.960	0.920
f1	**0.980**	0.961	0.950	0.949	0.970	0.939

The results of the deep learning models in the case of cutting different wood species are shown in Table 3. The best performance was achieved by the MobileNetV2 deep learning network with an accuracy of 98%. The second-best performance was achieved by the ResNet deep learning network with an accuracy of 97%, followed by VGG 19 (96%), DenseNet and SqueezeNet (95%), and finally

Inception-V3 with an accuracy of 94%. In comparison to other research (Jegorowa et al. 2020, Swidiersky 2022), the performance results reported in this work for the developed deep learning models can be regarded as quite good. However, there were no comparable studies involving different wood species. Future research in this direction should include more wood species and more types of tools to substantiate the results presented in this paper. In addition, there is still room for investigation of the tool condition using the applied methodology as well as the sound wave propagation in the wood during cutting.

Table 4. *Performances of the developed deep learning models for different tool condition sound classification.*

	MobileNetV2	VGG19	DenseNet	SqueezeNet	ResNet	Inception_v3
Accuracy	**0.930**	0.85	0.9	0.89	0.91	0.87
Precision	**0.921**	0.830189	0.857143	0.882352941	0.886792	0.862745
Recall	**0.940**	0.88	0.96	0.9	0.94	0.88
f1	**0.930**	0.854359	0.90566	0.891089109	0.912621	0.871287

According to Table 4, deep learning models provided satisfactory results in recognising the tool state. The accuracy of tool wear detection varied from 85% for the DenseNet network to 93% for MobileNet V2. The values shown in Table 3, especially the accuracy, are slightly lower than the tool type detection (97.5%), but can be considered significant as they are caused by small changes in teeth geometry.

5. CONCLUSION

The methodology presented in this paper offers good prospects for noise detection as a tool for monitoring the machining process, leading to smart machining as part of Industry 4.0 and beyond.

The right choice of frequency range, signal processing and data preparation, together with the application of a neural network, can provide an answer to the machining process, material and tool.

In this article, it is shown that the noise generated by the use of a circular saw, whether it is interacting with the material or just idling, can provide enough information for process monitoring.

After all that has been said before, one could come to the conclusion:

- The sound signal investigated in this study proves to be a satisfactory data carrier for this type of investigation;
- The processing of the sound signal provided quite good information that is consistent with certain circular saw blades;
- From the average spectral density plots, it was quite clear which spectral regions were of interest for training the deep learning network;
- The spectrograms provided a sufficiently good basis as data for the deep learning process;
- According to the results of the deep learning networks, a validation accuracy of 100, 97.5, 98 and 93% was achieved, proving that this approach can be used for monitoring cutting processes in terms of decision-making;
- However, the results presented relate to the particular environmental conditions. No reverberation noise was taken into account;
- Further research in this area will include the interaction of a tool (circular saw blade) with other, more homogeneous materials commonly used in woodworking, with different cutting conditions and different degrees of bluntness of the tool.

Acknowledgement

This research was funded by the Ministry of Science, Technological Development and Innovation of the Republic of Serbia, under registration number 451-03-65/2024-03/200169, dated 05.02.2024.

REFERENCES

1. Abellan-Nebot J. V. Subirón F. R. (2010) “A review of machining monitoring systems based on artificial intelligence process models”, The International Journal of Advanced Manufacturing Technology, 47(1–4), 237–257, DOI: 10.1007/s00170-009-2191-8
2. Aguilera A. (2011) “Cutting energy and surface roughness in medium density fibreboard rip sawing”, *European Journal of Wood and Wood Products*, 69(1), 11-18. DOI: 10.1007/s00107-009-0396-z
3. Aguilera A. (2011a) “Surface roughness evaluation in medium density fibreboard rip sawing”, European Journal of Wood and Wood Products, 69(3), 489-493. DOI:10.1007/s00107-010-0481-3
4. Aguilera A. Barros J. L. (2010) “Sound pressure as a tool in the assessment of the surface roughness on medium density fibreboard rip sawing process”, Maderas. Ciencia y tecnologia, 12(3), 159–169, DOI:10.4067/S0718-221X2010000300001
5. Aguilera A. Rolleri A. Burgos F. (2016) “Cutting distance as factor to evaluate the quality of wood machined surfaces: A preliminary study”, Maderas, Ciencia y tecnologia vol.18 no.1, doi.org/10.4067/S0718-221X2016005000001
6. Aguilera A. Zamora R. (2007) “Wood machining process monitoring of blackwood (Acacia melanoxylon) with acoustic emission technique and his relationship with resulting surface roughness”, Maderas: Ciencia y Technologia, 2007, 9(3), 323-332, doi.org/10.4067/S0718-221X2007000300011
7. Brémaud I. El Kaïm Y. Guibal D. Minato K. Thibaut B. Gril J. (2012) “Characterisation and categorisation of the diversity in viscoelastic vibrational properties between 98 wood types”, Annals of Forest Science 69(3), DOI: 10.1007/s13595-011-0166-z
8. Cyra G. Tanaka C. (2000) “The effects of wood-fibre directions on acoustic emission in routing”, Wood Science and Technology, 34, 237–252.
9. de Geus, A.R., da Silva, S.F., Gontijo, A.B., Silva, F.O., Batista, M.A., Souza, J.R. (2020) “An analysis of timber sections and deep learning for wood species classification”, Multimedia Tools and Applications, 79, 34513–34529, DOI: 10.1007/s11042-020-09212-x
10. Dünisch O. (2017) “Relationship between anatomy and vibration behaviour of softwoods and hardwoods”, IAWA Journal, 38(1), 81-98, DOI: 10.1163/22941932-20170158
11. Goli G. Curti R. Marcon B. Scippa A. Campatelli G. Furferi R. Denaud L. (2018) “Specific Cutting Forces of Isotropic and Orthotropic Engineered Wood Products by Round Shape Machining”, Materials, 11(12): 2575, DOI: 10.3390/ma11122575
12. Goli G. Fioravanti M. Marchal R. Uzielli L. (2010) “Up-milling and down-milling wood with different grain orientations - Theoretical background and general appearance of the chips”, European Journal of Wood and Wood Products, 67(3):257-263, DOI: 10.1007/s00107-009-0323-3
13. Iskra P. Hernández RE. (2009) “The influence of cutting parameters on the surface quality of routed paper birch and surface roughness prediction modelling”, Wood and Fiber Science, 41(1), 28–37.
14. Iskra P. Hernández RE. (2009) “The influence of cutting parameters on the surface quality of routed paper birch and surface roughness prediction modelling”, Wood and Fiber Science, 41(1), 28–37.
15. Iskra P. Hernández RE. (2012) “Toward a process monitoring of CNC wood router. Sensor selection and surface roughness prediction”, Wood Science and Technology, 46(1–3), 115–128, DOI: 10.1007/s00226-010-0378-7
16. Iskra P. Hernández RE. (2012) “Toward a process monitoring of CNC wood router. Sensor selection and surface roughness prediction”, Wood Science and Technology, 46(1–3), 115–128, DOI: 10.1007/s00226-010-0378-7
17. Iskra P. Tanaka C. (2005). “The influence of wood fibre direction, feed rate and cutting width on sound intensity during routing,” Holz als Roh-und Werkstoff 63, 167-172. DOI: 10.1007/s00107-004-0541-7

18. Iskra P. Tanaka C. (2005). “The influence of wood fibre direction, feed rate and cutting width on sound intensity during routing,” Holz als Roh-und Werkstoff 63, 167-172. DOI: 10.1007/s00107-004-0541-7
19. Jegorowa A. Kurek J. Antoniuk I. Dołowa W. Bukowski M. Czarniak P. (2020) “Deep learning methods for drill wear classification based on images of holes drilled in melamine faced chipboard”, Wood Science and Technology 55(1):1-23, DOI: 10.1007/s00226-020-01245-7
20. Jemielniak K. Urbański T. Kossakowska J. Bombiński S. (2011)” Tool condition monitoring based on numerous signal features”, Int J Adv Manuf Technol (2012) 59:73–81, DOI 10.1007/s00170-011-3504-2
21. Kibleur P. Aelterman J. Boone MN. Van den Bulcke J. Van Acker J. (2022) “Deep learning segmentation of wood fibre bundles in fibreboards”, Composites Science and Technology, 221, https://doi.org/10.1016/j.compscitech.2022.109287
22. Kováč J. Harvánek P. Krilek J. Kuvik T. Melicherčík J. (2021) “Analysis of cutting conditions in the process of cross-cutting wood by circular saws”, “Circular saw cross-cutting,” BioResources 16(1), 1029-1041. DOI:10.15376/biores.16.1.1029-1041
23. Mandic M. Svrzic S. Danon G. (2015) “The comparative analysis of two methods for the power consumption measurement in circular saw cutting of laminated particle board”, Wood Research 60 (1), 125-136.
24. Miric-Milosavljevic M. Svrzic S. Nikolić Z. Djurkovic M. Furtula M. Dedic A. (2024)” Signal Processing and Machine Learning as a Tool for Identifying Idling Noises of Different Circular Saw Blades”, BioResources, 2024, 19(1), 1744-1756, 10.15376/biores.19.1.1744-1756
25. Nasir V. Cool J. Sassani F. (2019) “Acoustic emission monitoring of sawing process: Artificial intelligence approach for optimal sensory feature selection”, *The International Journal of Advanced Manufacturing Technology* 102, 4179-4197. DOI:10.1007/s00170-019-03526-3
26. Nasir V. Sassani F. (2021) “A review on deep learning in machining and tool monitoring: methods, opportunities, and challenges”, The International Journal of Advanced Manufacturing Technology 115(2683–2709), DOI:10.1007/s00170-021-07325-7
27. Naylor A. Hackney P. Perera N. Clahr E. (2012) “Mechanical Cutting Force Model,” BioResources 7(3), 2883-2894., ISSN 1930-2126
28. Porankiewicz B. Axelsson B. Grönlund B. Marklund B. (2011) “Main and Normal Cutting forces by Machining Wood of Pinus Sylvestis”, BioResources 6(4), 3687-3713, DOI: 10.15376/BIORES.6.4.3867-3713
29. Stanojevic D. Mandic M. Danon G. Svrzic S. (2017) “Prediction of the surface roughness of wood for machining”, Journal of Forestry Research, 28(3), 1281–1283, DOI: 10.1007/s11676-017-0401-z
30. Sun Y. Lin Q. He X. Zhao Y. Dai F. Qiu J. Cao Y. (2021) “Wood Species Recognition with Small Data: A Deep Learning Approach”, International Journal of Computational Intelligence Systems,14(1),1451 – 1460, DOI: 10.2991/ijcis.d.210423.001
31. Svrzic S. Djurkovic M. Danon G. Furtula M. Stanojevic D. (2021) “On acoustic emission analysis in circular saw cutting beech wood with respect to power consumption and surface roughness,” *BioResources* 16(4), 8239-8257. DOI: 10.15376/biores.16.4.8239-8257
32. Szwajka K. Zielinska-Szwajka J. Gorski J. (2008) “Neural networks based in process tool wear prediction system in milling wood operations”, In International Symposium on Instrumentation Science and Technology (International Society for Optics and Photonics, 713312–713312, DOI: 10.1117/12.812090
33. Tanaka C. Nakao T. Nishino Y. Hamaguchi T. Takahashi A. (1992) “Detection of wear degree of cutting-tool by acoustic-emission signal”, Mokuzai Gakkaishi, 38(9), 841–846.
34. Tiryaki S. Malkoçoğlu A. Özşahin S. (2014) “Using artificial neural networks for modelling surface roughness of wood in machining process”, Construction and Building Materials, 66, 15, 329-335, doi.org/10.1016/j.conbuildmat.2014.05.098
35. Zafar T. Kamal K. Sheikh Z. Mathavan S. Jehanghir A. Ali U. (2015) “Tool health monitoring for wood milling process using airborne acoustic emission”, 2015 IEEE International

Conference on Automation Science and Engineering (CASE), Gothenburg, Sweden,1521–1526, DOI: 10.1109/CoASE.2015.7294315

36. Zbieć M. (2011) “Application of neural network in simple tool wear monitoring and identification system in MDF milling”, Drvna Industrija, 62(1), 43–54, doi.org/10.5552/drind.2011.1020